Desalination and Water Treatment
www.deswater.com
doi: 10.1080/19443994.2016.1178604

57 (2016) 26327–26335
November

Taylor & Francis
Taylor & Francis Group

Effect of microbubble generator operating parameters on oxygen transfer efficiency in water

Tekile Andinet[a], Ilho Kim[a,b,*], Jai-Yeop Lee[b]

[a]*Department of Construction Environment Engineering, University of Science and Technology, Daejeon 305-333, Republic of Korea, Tel. +82 10 4314 6822; email: andinetm@gmail.com (T. Andinet), Tel. +82 10 8728 6898; Fax: +82 31 910 0291; email: ihkim@kict.re.kr (I. Kim)*
[b]*Environmental and Plant Engineering Research Institute, Korea Institute of Civil Engineering and Building Technology (KICT), Goyang 411-712, Republic of Korea, Tel. +82 10 4525 9889; email: pas2myth@kict.re.kr (J.-Y. Lee)*

Received 4 January 2016; Accepted 11 April 2016

ABSTRACT

This study utilized multistage orifice microbubble generator to investigate dissolved oxygen (DO) formation characteristics and to increase its efficiency, by considering saturator pressure, water supply, and gas flow rates as the main operating factors. The effect of changing the parameters was described in terms of dissolution performance using volumetric mass transfer rate, which is very important element for aerator design and scale-up. Pressure values from 1 to 6 atm were taken for the analysis. To improve the oxygen transfer efficiency of the multistage orifice, the internal supply line was controlled to circulate the bubbles water up to 300% cycling. The volumetric mass transfer coefficient was limited below 0.01 per min for air; however, the value varied from 0.10 to 0.13 per min for oxygen at 4.5 L/min flow rate, showing increasing pattern with pressure. The transfer characteristic was doubled, with circulating ratio applied, because circulation could multiply the number of microbubbles. Examining the various operating conditions within the range set for the cost to generate 1 kg of DO, under gas injection velocity of 1.27 m/s, higher liquid pressurization showed lower cost per production in case of oxygen than air. Thus, natural water bottom area environment can be economically improved using oxygen microbubbles, considering the excessive dissolution.

Keywords: Microbubble; Dissolved oxygen; Operating parameters; Mass transfer; Cost-benefit

1. Introduction

Tsuge [1] stated microbubbles based on the working field as, 10–40 μm for bioactivity and less than 100 μm for fluid physics. The gases used for generating microbubbles include air as well as hydrogen [2], oxygen [3], and ozone [4–6] based on the use and characteristics. Air and oxygen are used for establishing aerobic environments in waters under anaerobic or hypoxic conditions [7–9]. These gases are also used

*Corresponding author.

Presented at CEST2015—14th International Conference on Environmental Science and Technology, Rhodes, Greece, 3–5 September 2015

in separation processes to absorb and float pollutants to the water surface; hence, their application in water quality control and water treatment fields such as river or lake [9], sewage treatment [10], and to purify leachate from waste-dumped landfills [11] is being extended gradually.

In Korea, as natural lakes are limited in number and small in size, a large number of water storage reservoirs are constructed to meet freshwater demand of the society [12]. However, the reservoirs created large zones of dead water, and in consequence, they suffered from water quality troubles due to eutrophication [13,14]. To control eutrophication, intervention measure such as aeration of the water body is necessary until changes in catchment management practices result in reduced input of nutrients [15]. Some aerators have already been installed; nevertheless, most of them supply quite coarse air bubbles which rise rapidly, burst on the water surface and hence inefficient in gas transfer [16,17].

Alternatively, if microbubbles, which have characteristics such as large gas–liquid interfacial area and extremely slow rising velocity, are used, the oxygen transfer to water will be facilitated. And, in controlling eutrophication, hypolimnetic aeration is preferred to destratification due to its ability to selectively oxygenating the hypolimnion of stratified lakes and reservoirs, while maintaining thermal stratification. This can be effectively achieved using microbubbles which show limited vertical mixing. Besides, by choosing appropriate type of gas, oxygen transferred to hypolimnetic water can be optimized.

In this study, pressurized microbubble generator was used to examine the influence of the microbubble generator operating parameters on dissolved oxygen (DO) formation, with a specific focus on the oxygen mass transfer (K_La) from bubbles to surrounding water. K_La is most important parameter for design and scale-up of aerators [18]. Impacts of type and velocity of injection gas, supply velocity of mixed liquid. and circulating rate of generated microbubbles water on oxygen transfer efficiency were examined. Supposing the same size mechanical devices for initial cost, the system running cost-benefit for the different operating scenarios was also analyzed based on the amount of gas transfer per unit time.

2. Materials and methods

2.1. Experimental apparatus and test conditions

When water is introduced into a pump, the water velocity becomes extremely high compared to that at the exit, thus causing the pressure at downstream of the body become quite low. Due to the difference in pressure, air is automatically sucked through the small orifice drilled on the wall (Bernoulli's principle), and the air sucked is broken into a huge number of microbubbles by multistage orifice of the generator. Oxygen gas (99.99% purity, KUM OH Gas Co. Ltd, Korea) was supplied from the high-pressure cylinder through the pressure control. The bubbles with the water are guided to a saturator (also called nozzle or separator) where the air is effectively mixed with water and pressure is properly produced before passing to the cylindrical reactor where the bubbles supply the oxygen. The saturator was a cylindrical stainless steel having height of 0.5 m and diameter 0.3 m. Excess gas was exhaled from a release valve on the top of the separator. The experimental equipment was designed in such a way that the generated microbubble water was conveyed to the water tank and then flow back to the generator for circulation.

Fig. 1 shows the pressurized microbubble generator. The mixture of liquid and gas is pressurized in the tank, where the gas is dissolved at the saturation concentration. The pressure in the pressurized tank affects the size and number of the microbubbles. The pump had specification of 35 L/min flow rate, 37 m head, and 1.5 kWh power consumption. The experiment was conducted in the cylindrical reactor made of transparent acrylic with diameter 0.60 m and height 1.0 m. About 200 L volume of circulating water is kept in the tank. Water was supplied from a pump to the microbubble generator via a flow control valve and a flow meter for the liquid flow rate measurement. The gas suction rate into the microbubble generator was measured with a flow meter.

The microbubbles were generated in tap water of initial DO concentration in the range of 6.4–7.0 mg/L. The water flow rate into the reactor was 20 L/min, and gas flow rate of 1.5, 3.0, and 4.5 L/min was considered as operating condition. The gas operating pressures of 2.5, 3.5, and 4.5 atm were used. The size

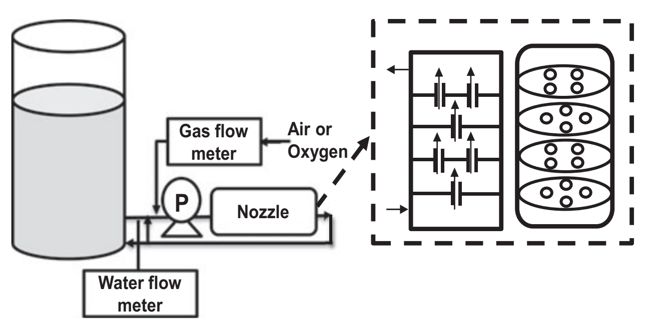

Fig. 1. Schematic diagram of the bubble generator.

of microbubble is related to the velocity of fluid which causes cavitation, and it is inversely proportional to the pressure in the range of 2.5 and 4.0 atm, and it is relatively similar in other ranges [19]. Hence, the velocity of the fluid flowing at rate of 0.85, 1.02, and 1.19 m/s corresponds to pressure of 2.5, 3.5, and 4.5 atm, respectively. Image analysis, which consisted of a measuring cell, a digital camera, a microscope, and a computer for image processing, was used to measure the bubble sizes. The average bubble size varied from 28 to 100 μm.

Meanwhile, the microbubble water was taken from the supply tank to the water tank and flowing it again through the orifice nozzles for multistage effect. In this experiment, the pipe lineup of the experimental equipment was manipulated to create higher DO concentration by circulating generated microbubble water to the water tank at 100, 200, and 300%. To check the effect of circulating rate on the improvement of DO, only gas injection velocity at 1.27 m/s (1.5 L/min) and liquid supply velocity at 1.19 m/s were considered. And to check the difference in the DO concentration according to the circulating rate, the DO concentration was measured at 0.1, 0.3, and 0.7 m position from the tank floor level.

2.2. Volumetric mass transfer measurement

At the outset of the experiments, nitrogen gas (99.9% purity, KUM OH Gas Co. Ltd, Korea) was blown into the water so as to reduce the already DO content to about 4 mg/L because the tap water showed a high DO value. Reduction only up to 4 mg/L was considered because it required very long time to reduce to zero [3]. Then, natural air or oxygen gas was fed into the water through the microbubble generator at desired flow rates of gas and the liquid at the bottom of the reactor. The time variation of the oxygen concentration, C, in the reactor water, was measured with a DO meter (Orion Star A223 RDO, Co.) at 30 cm depth from the bottom of the tank.

Since temperature affects gas solubility, its measurement (24–27˚C) was taken along with DO. The variation is actually used as correction factor for oxygen solubility [20]. In this study, the DO meter employed automatically converted values of DO at measurement temperature to their equivalent values at the standard temperature of 20˚C and pressure 1 atm. From the time variation data of C, the volumetric mass transfer coefficient at temperature T, $K_L a_T$, was determined by the integrated form of the model for non-steady state test:

$$K_L a_T = \frac{\ln[(C_s - C_1)/(C_s - C_2)]}{t_2 - t_1} \tag{1}$$

Here, C_s is the DO concentration at equilibrium condition, t_1 and t_2 are times chosen at which measured oxygen concentrations, C_1 and C_2, are 20% (t_1) and 80% (t_2), respectively, of the saturation values for the test water [18]. Plotting Eq. (1) on semilog scale, $K_L a$ is estimated provided that C_s is known from DO vs. time plot.

Based on the dissolution of the gas amount to the water, the operational costs of oxygen and natural air are compared under the operation factors. For this, gas material and power consumption, which are the first and second terms, respectively, of the nominator in Eq. (2), are determined. Mass of oxygen transferred per unit time (O_s) was determined by multiplying $K_L a$ with the DO concentration at saturation (C_s) for the standard conditions and volume, V, of water in the tank. The O_s varies with the operating factors as it depended on $K_L a$:

$$C = \frac{(C_0\ Q_0) + (\text{P.C.}\ C_e\ T)}{O_s} \tag{2}$$

where C is the operation cost (KRW/kg DO); C_0 is the oxygen gas cost (KRW/L); Q_0 is the oxygen flow rate (L/min); P.C. is the power consumption of pump (kWh); C_e is the electricity cost (KRW/kWh); T is the pump operation time (min); and O_s is the amount of DO supply (kg DO). KRW is Korean republic currency (1 US \$ is about 1,100 KRW).

3. Results and discussions

3.1. Effect of the operating parameters on DO concentration and mass transfer

There was no distinct correlation of the DO concentration variation with both the liquid supply velocity and gas injection velocity, using air. Fig. 2 shows DO concentration changing with time for each injection velocity of oxygen gas. The higher the velocity, more significant the change became. In the same gas injection velocity, DO formation increased proportionally due to rise in the liquid supply velocity. However, this trend somewhat changed as the gas injection velocity increased, and as shown in Fig. 2(b) and (c), when the gas injection velocity increased, there was a slight change in the liquid velocity at 1.02 and 1.19 m/s, specially until 20 min. When the gas injection velocity increased further, there was little

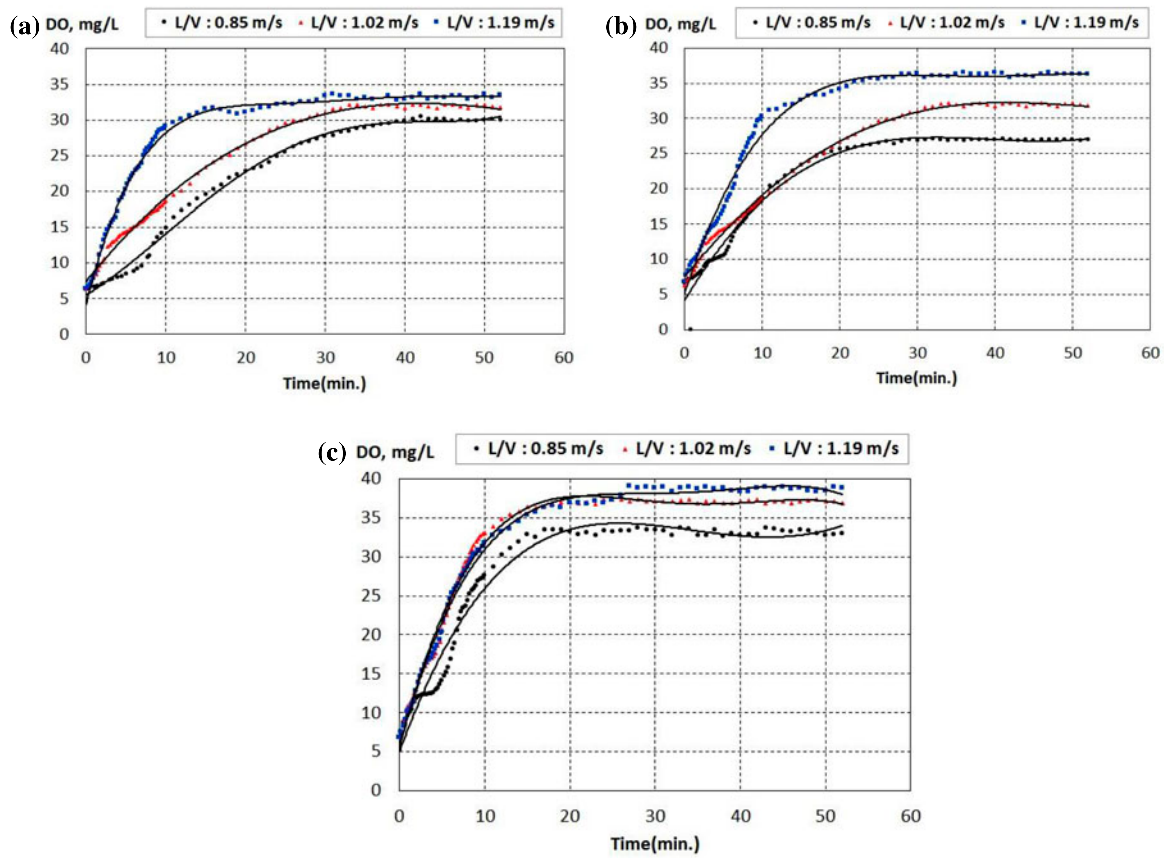

Fig. 2. Transient DO concentration profiles at various oxygen supply velocity: (a) 1.27 m/s, (b) 2.55 m/s, (c) 3.82 m/s (L/V refers to liquid velocity).

influence on oxygen due to the difference in the liquid velocity.

In the beginning, the average increases in DO were 0.772, 1.135, and 2.394 DO/min according to the supply velocity at the injection velocity of 1.27 m/s, showing a clear difference. For the oxygen injection velocity of 2.55 m/s, by increasing the liquid supply rate from 0.85 to 1.02 m/s, there was a significant effect on the DO rate; however, further increasing the liquid flow rate to 1.19 m/s, there was almost no improvement. In other words, as the oxygen gas injection velocity increased, the influence according to the liquid supply rate decreased gradually so that when the injection velocity was 3.82 m/s, the change in DO rate did not show considerable variation.

The reaction velocity increased based on the supply velocity due to the impact of the bubble size. Han et al. [19] demonstrated that the average bubble size decreases from 54 to 30 μm when the liquid pressure is increased from 2.5 to 3.5 atm, depicting linear inverse proportionality. Therefore, it is deduced that the supply velocity in the operating conditions was related to the pressure, influencing the size of bubbles generated so that by increasing the supply velocity, the size of bubble became smaller. When the size of bubble is small, the specific surface area becomes larger. Hence, it is expected that the oxygen transfer efficiency from bubble to liquid will get enhanced.

The DO saturated concentration with air was 10.17–10.93 mg/L, while it could be raised to 27.09–39.22 mg/L using oxygen (Table 1), showing an average difference of more than three times between air and oxygen. Henry's law, which explains that the dissolved concentration is proportional to the partial pressure of gaseous phase, is the ground for the variation [21]. It is also considered as temporary dissolution effect by residence of air microbubbles supplied continuously. Actually, DO concentration slowly decreased after the generation of microbubbles, in comparison with the saturating concentration at the time of generating microbubbles. This is because a high dissolution effect is shown temporarily as

Table 1
The saturated concentrations by the experimental factors

		Liquid velocity (m/s)		
Gas velocity (m/s)		0.85	1.02	1.19
Air	1.27	10.17	10.18	10.17
	2.55	10.58	10.57	10.45
	3.82	10.81	10.93	10.71
Oxygen	1.27	30.46	32.15	33.65
	2.55	27.09	35.27	36.55
	3.82	33.69	37.52	39.22

increase in the solubility due to microbubble water supplied continuously offsets effects such as bubble extinction or liftoff when generating microbubbles.

In order to evaluate the DO concentration generation and transfer characteristics more quantitatively, oxygen transfer coefficient was calculated based on the oxygen transfer model for aerators, described in Eq. (1). The oxygen transfer coefficients were deduced from experimental DO concentration in the plot vs. time (Fig. 3). For instance, at gas velocity of 3.82 m/s and liquid velocity of 1.19 m/s, the saturation or near saturation DO concentration, C_s, is 39.22 since almost constant value was attained. Considering this C_s value, the best fit line for the plot based on Eq. (1) is given by, is $C = 0.1286t$ at $R^2 = 97.44\%$ (Fig. 3(b)); hence, K_La was estimated to be 0.1286.

Thus, oxygen solubility as aeration performance assessment was determined by DO saturation concentration measurement with time elapse. The corresponding oxygen transfer capacity coefficient or transfer rate was used then to compare the different operating pressures and flows considered.

The oxygen transfer coefficients for all the experimental factors are shown in Fig. 4. In the case of using air as the injection gas, the oxygen transfer coefficient was 0.004–0.006 min^{-1}, showing that there was no significant influence by the factors. However, the mass transfer of oxygen is extremely higher than that of air; specifically, the value at 4.5 atm and 3.82 m/s flow rate (0.13 min^{-1}) was 28 times higher. Leu et al. [22] have given explanation to similar result, stating that the resistance of liquid vapor interface was reduced due to fast gas supply. And in this study, it was due to the increase in the amount of air supply rather than the reduction of resistance taking into account the principle of microbubble generation. When the gas velocity is high, the amount of gas injection becomes larger so that gas and air fraction ratio in the gas–liquid mixture increases and when cavitation occurs in the nozzle, proper oxygen can be provided. This means that more opportunities are created to absorb required oxygen from gas–liquid mixture when microbubbles are generated.

3.2. DO concentration change characteristic by depth based on circulation rate

Microbubble water generated was stored in the water tank temporarily through the transfer line and then it was supplied to the generator together with gas using the pump to apply multistage orifice effect. The circulating rate was adjusted to 100, 200, and 300% by applying the number of return. The graphs in Fig. 5 are contour plots to depict vertical and lateral DO concentration variation with time, in reference to the injection point. The plots showed diffusion effect by monitoring points installed at constant intervals in the reactor tank. The extent of DO diffusion was examined by the spread of colors; with more circulation rate, there was more rapid diffusion to the upper area from bottom where the bubbles supplied. The

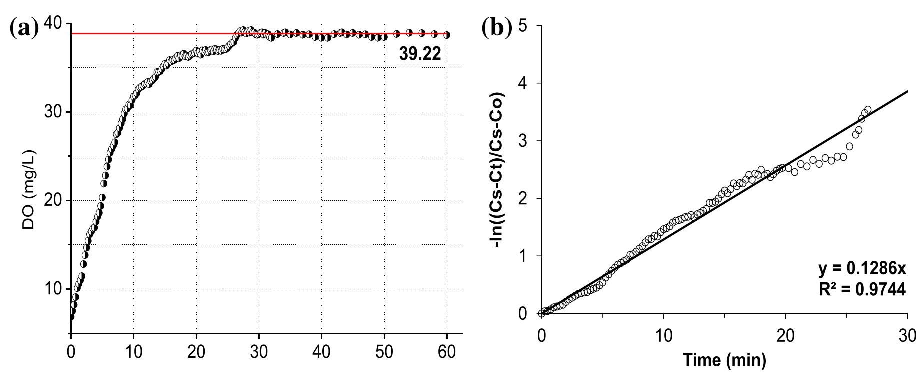

Fig. 3. (a) DO variation with time at gas velocity 3.82 m/s and liquid velocity 1.19 m/s and (b) a result of application for volumetric oxygen transfer model.

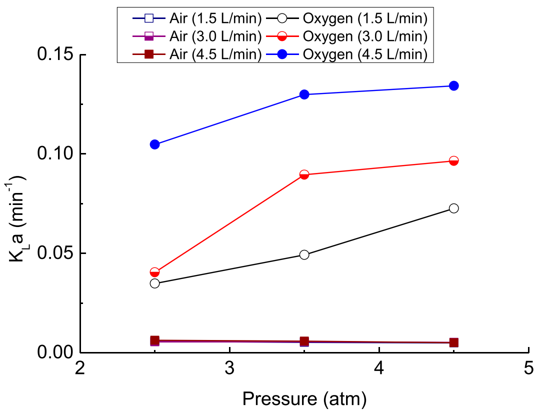

Fig. 4. Volumetric oxygen transfer coefficient for each operating condition.

blue color, which represented more DO, appeared in just 2 min in 300% circulation; however, 10 min was taken for the noncirculation case. The color change which means DO transfer from bubbles showed changing tendency with circulation increase.

Hence, the DO concentration changed in the microbubble water where circulating rate is applied according to the time and depth, and the concentration changes were in the range of 6–27 mg/L. From the graph, DO concentration increased from the lower level upwards gradually. On the other hand, in case of applying circulating rate, as the value increased, the transfer characteristic was improved.

The oxygen transfer characteristics due to circulation were evaluated quantitatively using the oxygen transfer coefficient K_La and presented in Table 2.

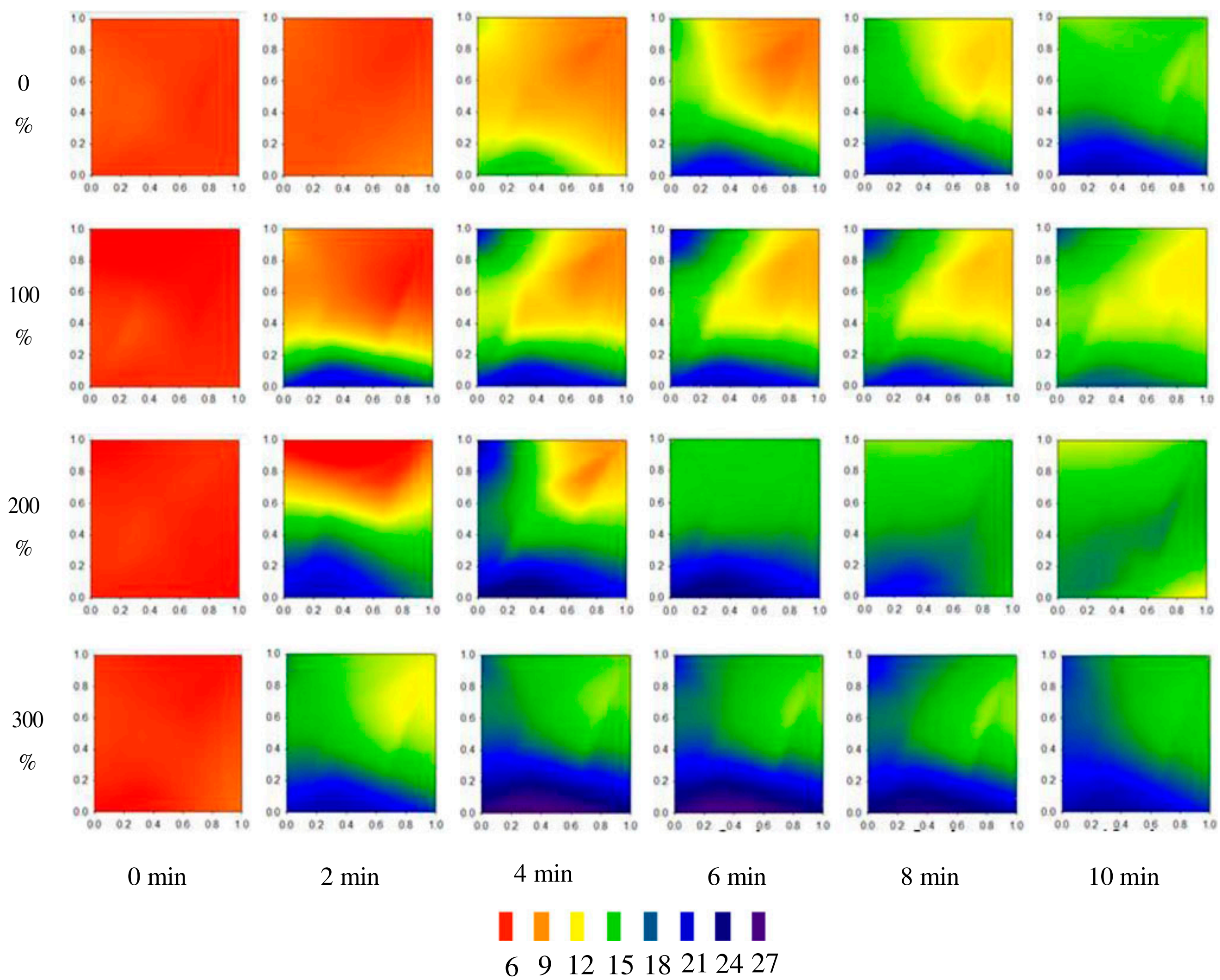

Fig. 5. Time variation of DO concentration by circulation rate and depth (x axis: width (m) and y axis: height (m)).

Table 2
The oxygen transfer characteristics (min^{-1}) by depth and circulation rate

	Circulation (%)			
Depth	0	100	200	300
Top	0.022	0.028	0.036	0.044
Middle	0.029	0.026	0.049	0.049
Bottom	0.058	0.089	0.119	0.139

The transfer characteristics due to increase in circulation rate showed a clear increasing trend, confirming that it had a significant effect in the microbubble generation and the oxygen transfer. Depending on the circulation rate, the transfer effect improved by twofold at 300% in reference to no circulation case. Kim [23] studied the characteristics of microbubbles generation using microbubble generator similar in principle with the one employed in this study. He confirmed that the microbubbles of a smaller size were generated in the structure with many obstacles, which corresponds to orifices in the orifice nozzle. The influence on the size of microbubbles took place in the same way as the operation control of the circulation, resulting in improved oxygen transfer characteristic.

For the water depth, the transfer characteristic of lower part was excellent since the line to supply microbubble is connected to the bottom, and the dissolution effect by the transfer capacity has become highest due to the characteristic of bubbles which were generated close to the supply time. Furthermore, as water depth increases, the hydrostatic pressure increases, and solubility also increases [22]. The effect of hydrostatic pressure due to water body in the reactor decreases when microbubbles lift off, so the oxygen transfer effect is reduced as microbubbles move upwards.

3.3. Evaluation of economic efficiency based on the operation cost

Gas material cost according to difference in the operating conditions and energy for the required pressure were converted into their equivalent economical values. The operation cost in comparison with DO generation was then obtained (Eq. (2)) by dividing the specific operation cost converted into economic figures based on the relevant DO supply amount of the operating conditions. Fig. 6 presents running cost-benefit comparison of air and oxygen under the considered operating conditions for only 20-min aeration.

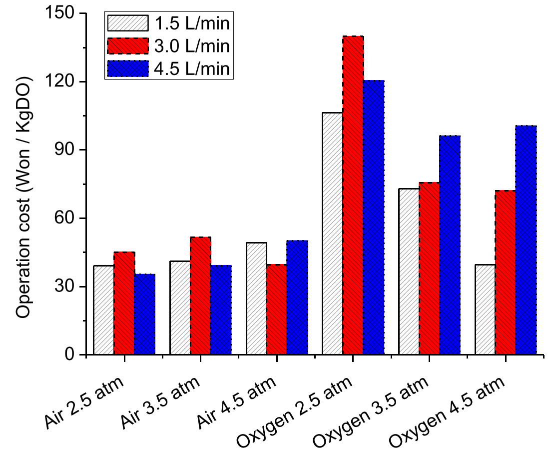

Fig. 6. Operation cost by each operating condition.

In case of air, the cost was 39 KRW/kg DO at the gas injection rate of 1.5 L/min and pressure of 2.5 atm, and for oxygen, the corresponding operation cost was 116 KRW/kg DO. However, at gas flow rate of 1.5 L/min and 4.5 atm liquid pressurization, use of oxygen is more economical than that of air. Generally, at higher pressure, which is followed by increase in DO, cost of oxygen gas per unit dissolution decreased. Besides, due to massive oxygen transfer (storage beyond certain level), practical oxygen aeration can be operated intermittently and hence saving running cost and contributing to service life of the facility.

4. Conclusions

In this study, it was intended to evaluate the influence of type of gas and its injection velocity to generate microbubbles, and the velocity of liquid supplied to dissolve the injected gas in microbubble generation and transfer characteristics. Besides, the effect of circulating the generated microbubble water was assessed as a way to improve the microbubble generation and transfer efficiency, and lastly, the economic efficiency of each operation methods was estimated and compared briefly on the assumption of actual field application. From the main results of the study, the following conclusions are drawn.

It was confirmed that gas type (air, oxygen), gas injection rate (1.5–4.5 L/min), and liquid supply velocity (0.85–1.19 m/s) selected as the factors influencing the generation of microbubbles showed difference in the bubble generation and oxygen transfer efficiency. In the case of air, there was no significant effect. However, when oxygen was used, gas injection velocity and liquid supply velocity improved DO amount as both gas and liquid flows increased. Each parameter had effect on solubility, amount, and size of microbubbles formed.

The effect of the parameters on oxygen transfer coefficient (K_La) was not recognized for air. But, in the case of oxygen, the K_La was enhanced up to 0.112 min^{-1}. The oxygen transfer effect became higher as the gas injection velocity and liquid supply rate improved.

By increasing the circulating rate of microbubble water from 0 to 300%, the generation of microbubbles and the DO concentration were improved by more than twice, in this study. Particularly, comparing the oxygen transfer effect of each water level, K_La value was improved from 0.058 to 0.139 min^{-1} at bottom levels. The number of microbubbles was duplicated by passing the already formed microbubble water through the multilevel orifice repeatedly. Considering the depth, the lower level where microbubbles were supplied showed 3 times higher transfer effect in comparison with the upper part. Hence, it is possible to use the mechanism for improving DO concentration of bottom part of water body, such as river or lake in the field application.

From the operational cost per dissolution of oxygen, there was significant difference depending on the operating conditions. By limiting the gas flow rate and increasing the pressure, more economical oxygen mass transfer was achieved using oxygen. In order to prepare the standard for determining economic efficiency, quantitative relationships regarding the quality, application purpose, and application effect of target water where microbubbles are applied should be analyzed more clearly.

Acknowledgement

This work is supported by the Korea Institute of Civil Engineering and Building Technology, KICT, of Korean Government number 2015-0113.

List of symbols

DO	—	dissolved oxygen
K_La	—	oxygen mass transfer coefficient
C_s	—	the DO concentration at equilibrium condition
t_1	—	time at which measured oxygen conc., C_1 is 20% of the saturation values for the test water
t_2	—	time at which measured oxygen conc., C_2 is 80% of the saturation values for the test water
C	—	operation cost (KRW/Kg DO)
C_0	—	oxygen gas cost (KRW/L)
Q_0	—	oxygen flow rate (L/min)
P.C.	—	power consumption of pump (kWh)
C_e	—	electricity cost (KRW/kWh)
T	—	pump operation time (min)
O_s	—	amount of DO supply (kg DO)
KRW	—	Korean republic currency (1 US $ is about 1,100 KRW)

References

[1] H. Tsuge, Micro- and Nanobubbles, Fundamentals and applications, Pan Stanford Publishing, USA, 2014.

[2] C. Ryu, J. Kim, D. Park, Y. Jung, Study on the behaivor of bubbles in the separators, Trans. Korean Hydrog. New Energy Soc. 23 (2012) 538–544.

[3] M. Sadatomi, A. Kawahara, H. Matsuura, S. Shikatani, Micro-bubble generation rate and bubble dissolution rate into water by a simple multi-fluid mixer with orifice and porous tube, Exp. Thermal Fluid Sci. 41 (2012) 23–30.

[4] P. Li, H. Tsuge, Ozone transfer in a new gas-induced contactor with microbubbles, J. Chem. Eng. Jpn. 39 (2006) 1213–1220.

[5] L.B. Chu, X.H. Xing, A.F. Yu, Y.N. Zhou, X.L. Sun, B. Jurcik, Enhanced ozonation of simulated dyestuff wastewater by microbubbles, Chemosphere 68 (2007) 1854–1860.

[6] P. Li, H. Tsuge, K. Itoh, Oxidation of dimethyl sulfoxide in aqueous solution using microbubbles, Ind. Eng. Chem. Res. 48 (2009) 8048–8053.

[7] K. Michioku, Y. Sakatani, K. Matsuo, T. Oda, Y. Hara, Reservoir purification by using micro-bubble aerator, The 7th Int. Conference on Hydroscience and Engineering, Philadelphia, September 10–13, 2006.

[8] S. Srithongouthai, A. Endo, A. Inoue, K. Kinoshita, M. Yoshioka, A. Sato, T. Iwasaki, I. Teshiba, H. Nashiki, D. Hama, H. Tsutsumi, Control of dissolved oxygen levels of water in net pens for fish farming by a microscopic bubble generating system, Fish. Sci. 72 (2006) 485–493.

[9] M. Sadatomi, A. Kawahara, K. Kurogawa, T. Akasaki, Purification of deep water in a Dam Lake using microbubbles and/or eco-bio-ring, Int. J. Environ. Sci. Dev. 6 (2015) 419–424.

[10] P. Li, Development of Advanced Water Treatment Technology using Microbubbles, PhD Dissertation, Keio University, Japan, 2006.

[11] K. Michioku, Microbubble aeration of polluted leachate from a landfill, Proceedings of 33rd IAHR Water Congress, Vancouver, BC, Canada, August 9–14, 2009.

[12] Y.J. Cha, M.P. Shim, S.K. Kim, The Four Major Rivers Restoration Project, UN Water International Conference, Zaragoza, Spain, June 2012.

[13] H.K. Bae, The effect of river flow retardation on algal growth, Nat. Resour. Conserv. 1 (2013) 30–34.

[14] L. Liu, D. Liu, D.M. Johnson, Z. Yi, Y. Huang, Effects of vertical mixing on phytoplankton blooms in Xiangxi Bay of Three Gorges Reservoir: Implications for management, Water Res. 46 (2012) 2121–2130.

[15] A. Tekile, I.H. Kim, J.S. Kim, Mini-review on river eutrophication and bottom improvement techniques,

with special emphasis on the Nakdong River, J. Environ. Sci. 30 (2015) 113–121.
[16] W.M. Heo, B. Kim, The effect of artificial destratification on phytoplankton in a reservoir, Hydrobiologia 524 (2004) 229–239.
[17] K.H. Oh, D.H. Jeong, S.Y. Yang, T.W. Jeon, Y.C. Cho, Effects of submerged aerator on the growth of algae in Daechung reservoir, J. Korean Soc. Environ. Eng. 35 (2013) 268–275.
[18] K.I. Ashley, K.J. Hall, D.S. Mavinic, Factors influencing oxygen transfer in fine pore diffused aeration, Water Res. 25 (1991) 1479–1486.
[19] M. Han, Y. Park, J. Lee, J. Shim, Effect of pressure on bubble size in dissolved air flotation, Water Sci. Technol. 2(5–6) (2002) 41–46.
[20] M.E. Lewis, Dissolved oxygen (ver. 2.0): U.S. Geological Survey Techniques of Water-Resources Investigations, Book 9, Chap. A6, 2006, pp. 35–37.
[21] I. Fandriks, Alternative methods for Evaluation of Oxygen Transfer Performance in Clean Water, Master dissertation, Uppsala University, Uppsala, 2011.
[22] H.G. Leu, S. Lin, C. Shyu, C. Lin, Effects of surfactants and suspended solids on oxygen transfer under various operating conditions, Environ. Technol. 19 (1998) 299–306.
[23] T.I. Kim, Analysis of Bubble Potential Energy and Its Application to Disinfection and Oil Washing, Doctoral Dissertation, Seoul National University, Seoul, 2010.